



Published in final edited form as:

Biol Blood Marrow Transplant. 2017 January ; 23(1): 30–37. doi:10.1016/j.bbmt.2016.10.022.

Therapeutic Effects of a NEDD8-Activating Enzyme Inhibitor, Pevonedistat, on Sclerodermatous Graft-versus-Host Disease in Mice

Chien-Chun Steven Pai^{1,†}, Lam T. Khat^{1,†}, Mingyi Chen², William J. Murphy^{1,3,*}, and Mehrdad Abedi^{3,‡}

¹Department of Dermatology, School of Medicine, University of California, Davis, Sacramento, California

²Department of Pathology, School of Medicine, University of California, Davis, Sacramento, California

³Department of Internal Medicine, School of Medicine, University of California, Davis, Sacramento, California

Abstract

Allogeneic hematopoietic stem cell transplantation (allo-HSCT) is the ultimate treatment for highly malignant hematologic disease; however, the major complication—graft-versus-host disease (GVHD)—still hinders its clinical application. In addition, chronic GVHD remains the major cause of long-term morbidity and mortality after allo-HSCT. Previously we showed that bortezomib, a proteasome inhibitor, can ameliorate the sclerodermatous GVHD response while maintaining graft-versus-tumor (GVT) effects. Here we report that pevonedistat (MLN4924), an inhibitor of the Nedd8-activating enzyme, which functions upstream of the proteasome in the ubiquitin-proteasome pathway, can also show similar protective effects. Recipient mice treated with pevonedistat demonstrated inhibitory effects on sclerodermatous GVHD pathogenesis. The beneficial effect of pevonedistat was observed to be temporally dependent, however. Whereas treatment given at the time of allo-HSCT administration or before the onset of symptoms worsened the scleroderma response, therapeutic administration starting at 20 days post-transplantation ameliorated the sclerodermatous GVHD. Flow cytometry analysis revealed differential effects on immune subsets, with inhibition of only antigen-presenting cells and not of donor T cells. Finally, pevonedistat preserved GVT effects in a sclerodermatous murine model of B cell lymphoma. Taken together, these data suggest that inhibition of neddylation with pevonedistat can serve as an alternative approach for the treatment of GVHD while maintaining GVT effects in a murine model of sclerodermatous GVHD.

* Correspondence and reprint requests: William J. Murphy, PhD, Department of Dermatology, internal Medicine, School of Medicine, Comprehensive Cancer Center, University of California, Davis, Sacramento, CA 95817.

† C.S.P. and L.T.K. contributed equally as first authors.

‡ M.A. and W.J.M. contributed equally as senior authors.

The content is solely the responsibility of the authors and does not necessarily represent the official views of the National Cancer Institute or the National Institutes of Health.

Conflict of interest statement: M.A. received partial research funding from the Millennium Company, and is on the speaker list of the Millennium Company for multiple myeloma. The other authors declare no competing financial interests.

Keywords

Pevonedistat; Sclerodermatous graft-versus-host disease; Graft-versus-tumor effect

Introduction

Allogeneic hematopoietic stem cell transplantation (allo-HSCT) remains the sole curative option for certain hematologic diseases; however, high incidences of graft versus-host-disease (GVHD) and tumor relapse are major hurdles associated with this approach [1]. Although recent advances in transplantation preparation and prophylactic regimens have reduced the incidence of acute GVHD (aGVHD), chronic GVHD (cGVHD) remains a major cause of long-term morbidity and mortality [2]. Recent studies suggest that inhibitors of various post-translational modifications (PTMs) may serve as therapeutic targeting agents for aGVHD pathogenesis [3,4]. The PTMs of proteins represent an important biochemical process that confers biochemical alterations, such as acetylation, phosphorylation, and ubiquitination [5]. Targeting PTMs by using small-molecule inhibitors has demonstrated potent antitumor effects [6-8], as well as immunomodulatory properties [3,5]. We have previously shown that bortezomib, a proteasome inhibitor that interferes with the degradation of ubiquitinated proteins, can successfully ameliorate sclerodermatous cGVHD responses in both preclinical and clinical studies [9]. In the present study we sought to investigate the effect of pevonedistat, an inhibitor of the NEDD8-activating enzyme (NAE), which functions upstream of the proteasome in the ubiquitin-proteasome pathway, on sclerodermatous GVHD in a murine model.

Pevonedistat is a selective inhibitor of the NEDD8-activating enzyme and inhibits the neddylation and activity of the cullin-RING ubiquitin ligases [10]. Thus, pevonedistat prevents the ubiquitination and degradation of a subset of proteins normally degraded by the proteasome. Pevonedistat exhibits antitumor effects in preclinical xenograft models of solid tumors and hematologic cancers, including acute myelogenous leukemia and lymphoma models [11-13]. Moreover, pevonedistat can suppress dendritic cell functions, such as the production of proinflammatory cytokines during allogeneic responses, suggesting that it may have therapeutic potential in allo-HSCT [3]. Given pevonedistat's inhibitory effects on immune subsets and cytokine regulations, we sought to examine its therapeutic effects on sclerodermatous GVHD responses. To investigate this, we used a minor MHC-mismatched murine model by transferring donor B10.D2 (H2^d) cells into BALB/c (H2^d) recipients. This is a well-established model of sclerodermatous cGVHD. We found that mice receiving pevonedistat starting on day 20 post-transplantation developed significantly less cGVHD compared with vehicle controls, whereas mice receiving early intervention regimens starting on day 0 or day 10 did not show protective effects on cGVHD. Flow data revealed that pevonedistat preferentially inhibited antigen-presenting cells (APCs), with less effect on donor-derived T cells. Finally, mice that received either vehicle or pevonedistat exhibited preserved graft-versus-tumor (GVT) effects when challenged with B cell lymphoma. Taken together, our data suggest that inhibition of the neddylation pathway with small molecules such as pevonedistat can provide an alternative approach for the treatment of sclerodermatous cGVHD in mice.

Materials and Methods

Mice and allo-HSCT

The 8- to 10-week-old B10.D2 mice used in these experiments were obtained from Jackson Laboratory, and 8- to 10-week-old female BALB/c mice were obtained from Taconic Farms. The BALB/c mice (H2^d) received lethal total body irradiation (800 cGy; ¹³⁷Cs source) and underwent transplantation from the donor B10.D2 mice (H2^d). T cell-replete bone marrow (BM) cells (8×10^6 cells) with or without spleen cells (25×10^6 cells) were injected i.v. through the tail vein into recipient mice. Mice injected with unfractionated spleen cells were then randomly allocated into different groups for further treatment. The mice were monitored for skin clinical scores and body weight loss twice weekly after allo-HSCT. Skin clinical score was assigned as described previously [14] as follows: 0, healthy appearance; 1, skin lesions with alopecia area $<1 \text{ cm}^2$; 2, skin lesions with alopecia area of 1 to 2 cm^2 ; 3, skin lesions with alopecia area $>2 \text{ cm}^2$. Tail, ear, or paw scaling represented an additional 0.3 point for each lesion. Mice with a clinical skin score >3.3 (on a scale of 0 to 3.9) or with severe ischemic tail lesions, severe diarrhea, or weight loss were euthanized. All mice were maintained at the University of California, Davis Medical Center's vivarium in accordance with Institutional Animal Care and Use Committee standards.

Reagents

Pevonedistat was dissolved in vehicle (10% 2-hydroxy-propyl-beta cyclodextrin) and injected i.p. at a dose of 20 mg/kg every 5 days starting at different time points. Pevonedistat was administered continuously until the end of the study period. As a positive control, bortezomib was injected at a dose of 0.1 mg/kg every 5 days starting at day +20 after allo-HSCT. The Cell Proliferation Assay Kit I (MTT) was purchased from Roche Diagnostics (Mannheim, Germany; catalog no. 11465007001), and used following the manufacturer's instructions.

Histology and histopathological scores

Tissues harvested from the mice were placed in 10% formalin, embedded in paraffin, sectioned, and stained with hematoxylin and eosin. Tissue sections were evaluated and graded by a board-certified pathologist in a single-blinded fashion. Skin pathology was scored on scale of 0 to 10 [14], based on dermal fibrosis (0 to 2), fat atrophy (0 to 2), inflammation (0 to 2), epidermal interface change (0 to 2), and follicular dropout (0 to 2). Gastrointestinal (GI) pathology was scored on a scale of 0 to 4, based on the extent of fibrosis and inflammation. Images were visualized with a Vanox AHBS3 microscope with an SPlan Apo 20 \times /0.70 NA objective (Olympus, Woodbury, NY). Images were acquired with a SPOT RT color digital camera using SPOT version 4.0.2 software (Diagnostic Instruments, Sterling Heights, MI).

Antibodies and flow cytometry analysis

Skin samples were prepared as described previously [15], and flow cytometry was performed as described previously [16]. In brief, single-cell suspensions (1 million cells) were first incubated with Fc Block (BD Pharmingen, San Diego, CA) for 10 minutes, then

coincubated with antibodies for 20 minutes at 4 °C, followed by washing with staining buffer (PBS + 1% FBS). Flow cytometry analysis was performed with an LSRFortessa cell analyzer (BD Biosciences, San Jose, CA), and data were analyzed using Flowjo software (Flowjo, Ashland, OR). CD19-FITC (BD Pharmingen), CD229.1-PE (BD Pharmingen), CD4-PE-Cy7 (eBioscience, San Diego, CA), CD25-APC-Cy7 (BD Biosciences), CD45-PB (BioLegend San Diego, CA), CD8 α -AF700 (BioLegend), B220-PE (BD Biosciences), CD138-PE (BioLegend), CD11c-FITC (BioLegend), F4/80-APC (eBioscience), and CD11b-APC-Cy7 (BioLegend) were used for these studies.

Bioluminescence imaging

The A20 (B cell lymphoma) cell line transfected with luciferase was injected i.v. into recipient BALB/c mice at a dose of 1×10^6 cells. Tumor cells were injected at day +20 after allo-HSCT as described above. Tumor growth was monitored with an IVIS Spectrum In Vivo Imaging System (PerkinElmer, Waltham, MA). In brief, mice were anesthetized with isoflurane and injected with D-luciferin (3 mg/mouse, i.p.), then imaged at 5 minutes postinjection with the IVIS Spectrum system. Bioluminescence data were analyzed using Living Image 3.0 (Caliper Life Sciences, Hopkinton, MA).

Statistics

Weight loss, skin clinical scores, and quantitative tumor burden were analyzed by 2-way analysis of variance (ANOVA) with Tukey's post hoc test for comparison among groups. Flow cytometry data were analyzed using the Student *t* test. A *P* value <.05 was considered significant. Survival curves were plotted on a Kaplan-Meier curve and analyzed by a log-rank test.

Results

Temporal-dependent effects of pevonedistat on sclerodermatous GVHD response

To investigate the therapeutic effects of NAE inhibition on sclerodermatous GVHD pathogenesis, we created a minor MHC mismatch murine model by transferring donor BM cells and splenocytes from B10.D2 (H2^d) donors into lethally irradiated BALB/c (H2^d) recipients. Recipient mice were then treated with pevonedistat (20 mg/kg i.p.) or vehicle control (10% 2-hydroxy-propyl-beta cyclodextrin i.p.) starting at different time points after allo-HSCT and continuing every 5 days thereafter until the end of the study (Figure 1A). Although body weight was not significantly different in the pevonedistat-treated groups at different administration time points compared with the vehicle-treated group (Figure 1C), the survival rate was better in mice that received pevonedistat treatment from day +20 (Figure 1D) owing to inhibitory effects on sclerodermatous responses.

We previously reported that bortezomib, a proteasome inhibitor, can inhibit sclerodermatous response during early, but not late, stages of sclerodermatous GVHD. Similarly, recipient mice treated with pevonedistat at the onset of cGVHD (day +20) demonstrated strong inhibition of sclerodermatous GVHD (Figure 1B and E); however, delayed treatment starting at day +35 did not provide any therapeutic effects (Figure 1F). Furthermore, mice treated with pevonedistat as prophylaxis initiated at either day 0 or day +10 after allo-HSCT either

worsened or did not exhibit any protective effects (Figure 1F). The temporal effects indicate that pevonedistat works only in a narrow time window during cGVHD pathogenesis, similar to the effects of bortezomib [9].

Pathological assessment confirmed that vehicle control group demonstrated typical sclerodermatous GVHD lesions, including epidermal thickening, increased fibrotic bands, and collagen deposition (Figure 2A, upper). Mice treated with pevonedistat from day +20 demonstrated ameliorated cutaneous sclerodermatous GVHD pathogenesis (Figure 2A, upper) and lower pathological scores (Figure 2B); however, pevonedistat had little effect on the GI tract, and mice treated with pevonedistat or vehicle exhibited dense fibrotic bands, severe ulceration and erosion, and local nonspecific inflammation with T cell infiltration in the GI tract as an aGVHD remnant (Figure 2A, lower and C). All mice had a score of 4 as the pathological readout despite treatments.

Pevonedistat specifically inhibits APCs but has less effect on T cells

It was previously reported that pevonedistat can regulate the antigen-presenting process by inhibiting canonical and noncanonical nuclear factor- κ B activities [3]. Given that APCs play significant roles in the skin GVHD response [17-19], we hypothesized that the amelioration of skin GVHD by pevonedistat seen in our experiments might have resulted from regulation of the antigen-presenting process. To investigate this possibility, mice treated with pevonedistat (starting at day +20 and continuing for every 5 days thereafter) or vehicle were harvested at day +59, and splenocytes were isolated and assayed by flow cytometry for different immune subsets. Ly9.1 (CD229.1) was used to distinguish recipient cells and donor-derived cells. Pevonedistat administration resulted in significant reductions in APCs, including dendritic cells (Figure 3A) and macrophages (Figure 3B). In addition, pevonedistat also reduced the number of donor-derived plasma cells despite the lack of inhibition of the number of B cells (Figure 3C and D). Although it reduced the number of APCs, pevonedistat demonstrated a minimal effect on T cells, with both donor CD4 (Figure 3E) and CD8 (Figure 3F) T cell numbers showing no significant difference compared with vehicle treatment groups.

Pevonedistat demonstrates less inhibitory effect on T cells compared with bortezomib

As we reported previously, both bortezomib and pevonedistat exhibited therapeutic effects on sclerodermatous GVHD pathogenesis; however, bortezomib can inhibit activated T cell proliferation [20], which potentially may hinder the GVT effects. To compare the effects of bortezomib and pevonedistat on T cell inhibition, splenocytes were isolated and stimulated with concanavalin A (2 μ g/mL) with either bortezomib or pevonedistat under different concentrations. Compared with pevonedistat, bortezomib exhibited a more potent inhibitory effect on T cell proliferation at the same concentration (Figure 4A and B), indicating that the lack of T cell inhibition from pevonedistat can potentially better preserve GVT effects and exert a smaller immunosuppressive effect on T cells.

Pevonedistat maintains GVT effects while decreasing sclerodermatous GVHD responses

Inhibition of antigen presentation and T cell activation can potentially hinder GVT effects and lead to tumor relapse. To further investigate whether pevonedistat may hinder GVT in

vivo, we challenged mice with a B cell lymphoma (A20) tumor model. Mice underwent allo-HSCT on day 0 and were challenged with B cell lymphoma on day +20, the time at which pevonedistat treatment was initiated (Figure 5A). To track tumors, we transfected B cell lymphoma with luciferase and monitored the mice using bioluminescence imaging. Whereas the mice receiving BM alone succumbed to a high tumor burden at around day 32 to 38, the mice receiving BM and pevonedistat treatment demonstrated decreased tumor burdens (Figure 5B and C). Administration of additional splenocytes elicited potent GVT effects, and administration of pevonedistat maintained and preserved GVT effects (Figure 5B and C). Despite the clear data presented in Figure 5B suggesting preservation of GVT effects by pevonedistat, no survival advantage could be demonstrated because in this particular model, pevonedistat did not prevent gut GVHD. There was no significant difference in weight loss between vehicle-treated and pevonedistat-treated groups that received BM cells and splenocytes with or without A20 cells (Figure 5D). In addition, mice receiving pevonedistat and splenocytes with tumors showed an ameliorated sclerodermatous GVHD response compared with mice receiving splenocytes with vehicle control and tumors (Figure 5E). These results indicate that pevonedistat can ameliorate sclerodermatous GVHD responses while maintaining GVT effects.

Discussion

We previously demonstrated that targeting proteasome with bortezomib can successfully inhibit sclerodermatous GVHD while maintaining GVT effects [9]. Compared with bortezomib, pevonedistat acts on a more upstream and more selective step in the ubiquitin-proteasome pathway by targeting the neddylation pathway that is required for the ubiquitin ligase activity of cullin-RING ligases, and also controls the stability of several cancer-related proteins [21,22]. The ability to target cancer-related pathways in GVHD treatment may allow for a direct antitumor effect while treating GVHD. Here we have shown that therapeutic administration of pevonedistat at the onset of GVHD pathogenesis can inhibit sclerodermatous response in mice; however, the effect is temporally dependent, similar to that of bortezomib. Prophylactic treatment immediately after transplantation may worsen the GVHD response, whereas delayed treatment after full establishment of sclerodermatous cGVHD might not provide a substantial therapeutic benefit, suggesting that both proteasome and NAE inhibitors work better in the early stages of sclerodermatous GVHD pathogenesis, at least in our murine model.

Two possibilities can explain the temporal-dependent effect of pevonedistat on cGVHD. First, regulatory B cells (Bregs) have been shown to secrete IL-10 and mediate tolerance in cGVHD pathogenesis [23]. Given that both immune proteasome and neddylation can affect the B cell population, prophylactic treatments may potentially hinder the formation of Bregs and accelerate cGVHD pathogenesis [23,24]. Second, bortezomib has been shown to induce GI tract toxicity through an increase in the number of TNF- α receptors and induction of acute GVHD-like lesions [25]. The inflammatory microenvironment in the GI tract during GVHD can have systemic effects on other target organs [26]; thus, it is likely that early GI tract inflammation induced by either bortezomib or pevonedistat in the early stages of cGVHD can lead to the development of skin GVHD. This was also evidenced by the greater in weight loss in mice receiving early intervention treatment (from day 0) with higher skin

GVHD clinical scores. The dual effects of either bortezomib or pevonedistat during different timing treatments suggest that clinical application requires careful evaluation.

Both bortezomib and pevonedistat demonstrated organ-specific effects, such that skin GVHD, but not GI GVHD, was ameliorated in this particular murine model. Organ-specific effects may be associated with the effects of neddylation pathways on donor T cells, particularly on chemokine receptor expression. We previously showed that inhibiting proteasome in T cell subsets with bortezomib can decrease CXCR3 expression on T cells [27], and CXCR3 has been shown to affect skin homing. Therefore, it is possible that neddylation also can affect the expression of chemokine receptors, resulting in organ-specific protection effects.

In terms of the antigen-presenting process during sclerodermatous GVHD, mice receiving pevonedistat demonstrate fewer reconstituting donor-derived APCs. In contrast, pevonedistat has only mild effects on T cell counterparts. The effect on APCs, but not on T cells, can minimize GVHD without jeopardizing the GVT effect, and also can decrease the risk of infection. Bortezomib can inhibit activated T cells, and pevonedistat may serve as an alternative molecular targeting agent for GVHD inhibition. Furthermore, a lack of T cell inhibition also may increase T cell reconstitution against opportunistic infections. Along with its immunomodulating effects, pevonedistat can preferentially inhibit tumor growth by targeting NAE within tumor cells, suggesting that it also can provide direct antitumor effects in addition to GVT effects.

With respect to clinical applications, although we observed therapeutic effects on the sclerodermatous GVHD response, whether pevonedistat can impact disease in any other GVHD target organs is unclear. Bortezomib is known to preferentially provide therapeutic effects in the skin, but not in the liver or GI tract [9,27]. We tested pevonedistat in a small range of dosages (data not shown), and the dosages and administration schedule need to be carefully evaluated for translation into clinical use. Overall, the NAE inhibitor pevonedistat demonstrated therapeutic effects on sclerodermatous GVHD responses in mice. Based on the recent data on its potential effect in patients with acute myelogenous leukemia and myelodysplastic syndrome [12,28], pevonedistat may have therapeutic potential in patients with these diseases post-transplantation and decrease the risk of sclerodermatous GVHD.

Acknowledgments

The authors thank Chanhyuk Park and John Ting Wei Huang for proofreading the manuscript.

Financial disclosure: This work was supported by National Cancer Institute Grant R01CA102282, and by research funding from the Millennium Company (to M.A.).

References

1. Blazar BR, Murphy WJ, Abedi M. Advances in graft-versus-host disease biology and therapy. *Nat Rev Immunol.* 2012; 12:443–458. [PubMed: 22576252]
2. Sarantopoulos S, Blazar BR, Cutler C, Ritz J. Reprint of: B cells in chronic graft-versus-host disease. *Biol Blood Marrow Transplant.* 2015; 21(2 Suppl):S11–18.
3. Mathewson N, Toubai T, Kapeles S, et al. Neddylation plays an important role in the regulation of murine and human dendritic cell function. *Blood.* 2013; 122:2062–2073. [PubMed: 23863900]

4. Magenau J, Reddy P. Next generation treatment of acute graft-versus-host disease. *Leukemia*. 2014; 28:2283–2291. [PubMed: 24938648]
5. Rabut G, Peter M. Function and regulation of protein neddylation “Protein modifications: beyond the usual suspects” review series. *EMBO Rep*. 2008; 9:969–976. [PubMed: 18802447]
6. Godbersen JC, Humphries LA, Danilova OV, et al. The Nedd8-activating enzyme inhibitor MLN4924 thwarts microenvironment-driven NF-kappaB activation and induces apoptosis in chronic lymphocytic leukemia B cells. *Clin Cancer Res*. 2014; 20:1576–1589. [PubMed: 24634471]
7. Luo Z, Yu G, Lee HW, et al. The Nedd8-activating enzyme inhibitor MLN4924 induces autophagy and apoptosis to suppress liver cancer cell growth. *Cancer Res*. 2012; 72:3360–3371. [PubMed: 22562464]
8. Gross S, Rahal R, Stransky N, et al. Targeting cancer with kinase inhibitors. *J Clin Invest*. 2015; 125:1780–1789. [PubMed: 25932675]
9. Pai CC, Chen M, Mirsoian A, et al. Treatment of chronic graft-versus-host disease with bortezomib. *Blood*. 2014; 124:1677–1688. [PubMed: 25009225]
10. Soucy TA, Smith PG, Milhollen MA, et al. An inhibitor of NEDD8-activating enzyme as a new approach to treat cancer. *Nature*. 2009; 458:732–736. [PubMed: 19360080]
11. Milhollen MA, Traore T, Adams-Duffy J, et al. MLN4924, a NEDD8-activating enzyme inhibitor, is active in diffuse large B-cell lymphoma models: rationale for treatment of NF- κ B-dependent lymphoma. *Blood*. 2010; 116:1515–1523. [PubMed: 20525923]
12. Swords RT, Erba HP, DeAngelo DJ, et al. Pevonedistat (MLN4924), a first-in-class NEDD8-activating enzyme inhibitor, in patients with acute myeloid leukaemia and myelodysplastic syndromes: a phase 1 study. *Br J Haematol*. 2015; 169:534–543. [PubMed: 25733005]
13. Khalife J, Radomska HS, Santhanam R, et al. Pharmacological targeting of miR-155 via the NEDD8-activating enzyme inhibitor MLN4924 (pevonedistat) in FLT3-ITD acute myeloid leukemia. *Leukemia*. 2015; 29:1981–1992. [PubMed: 25971362]
14. Anderson BE, McNiff JM, Matte C, et al. Recipient CD4⁺T cells that survive irradiation regulate chronic graft-versus-host disease. *Blood*. 2004; 104:1565–1573. [PubMed: 15150080]
15. Ginhoux F, Collin MP, Bogunovic M, et al. Blood-derived dermal langerin⁺ dendritic cells survey the skin in the steady state. *J Exp Med*. 2007; 204:3133–3146. [PubMed: 18086862]
16. Sun K, Wilkins DE, Anver MR, et al. Differential effects of proteasome inhibition by bortezomib on murine acute graft-versus-host disease (GVHD): delayed administration of bortezomib results in increased GVHD-dependent gastrointestinal toxicity. *Blood*. 2005; 106:3293–3299. [PubMed: 15961519]
17. Alexander KA, Flynn R, Lineburg KE, et al. CSF-1-dependant donor-derived macrophages mediate chronic graft-versus-host disease. *J Clin Invest*. 2014; 124:4266–4280. [PubMed: 25157821]
18. Johnston HF, Xu Y, Racine JJ, et al. Administration of anti-CD20 mAb is highly effective in preventing but ineffective in treating chronic graft-versus-host disease while preserving strong graft-versus-leukemia effects. *Biol Blood Marrow Transplant*. 2014; 20:1089–1103. [PubMed: 24796279]
19. Young JS, Wu T, Chen Y, et al. Donor B cells in transplants augment clonal expansion and survival of pathogenic CD4⁺ T cells that mediate autoimmune-like chronic graft-versus-host disease. *J Immunol*. 2012; 189:222–233. [PubMed: 22649197]
20. Sun K, Welniak LA, Panoskaltis-Mortari A, et al. Inhibition of acute graft-versus-host disease with retention of graft-versus-tumor effects by the proteasome inhibitor bortezomib. *Proc Natl Acad Sci USA*. 2004; 101:8120–8125. [PubMed: 15148407]
21. Milhollen MA, Thomas MP, Narayanan U, et al. Treatment-emergent mutations in NAEbeta confer resistance to the NEDD8-activating enzyme inhibitor MLN4924. *Cancer Cell*. 2012; 21:388–401. [PubMed: 22439935]
22. Soucy TA, Smith PG, Rolfe M. Targeting NEDD8-activated cullin-RING ligases for the treatment of cancer. *Clin Cancer Res*. 2009; 15:3912–3916. [PubMed: 19509147]
23. Khoder A, Sarvaria A, Alsuliman A, et al. Regulatory B cells are enriched within the IgM memory and transitional subsets in healthy donors but are deficient in chronic GVHD. *Blood*. 2014; 124:2034–2045. [PubMed: 25051962]

24. Zhang C, Todorov I, Zhang Z, et al. Donor CD4+ T and B cells in transplants induce chronic graft-versus-host disease with autoimmune manifestations. *Blood*. 2006; 107:2993–3001. [PubMed: 16352808]
25. Sun K, Li M, Sayers TJ, et al. Differential effects of donor T-cell cytokines on outcome with continuous bortezomib administration after allogeneic bone marrow transplantation. *Blood*. 2008; 112:1522–1529. [PubMed: 18539902]
26. Takashima S, Kadowaki M, Aoyama K, et al. The Wnt agonist R-spondin1 regulates systemic graft-versus-host disease by protecting intestinal stem cells. *J Exp Med*. 2011; 208:285–294. [PubMed: 21282378]
27. Pai CC, Hsiao HH, Sun K, et al. Therapeutic benefit of bortezomib on acute graft-versus-host disease is tissue specific and is associated with interleukin-6 levels. *Biol Blood Marrow Transplant*. 2014; 20:1899–1904. [PubMed: 25064746]
28. Shah JJ, Jakubowiak AJ, O'Connor OA, et al. Phase I study of the novel investigational NEDD8-activating enzyme inhibitor pevonedistat (MLN4924) in patients with relapsed/refractory multiple myeloma or lymphoma. *Clin Cancer Res*. 2016; 22:34–43. [PubMed: 26561559]

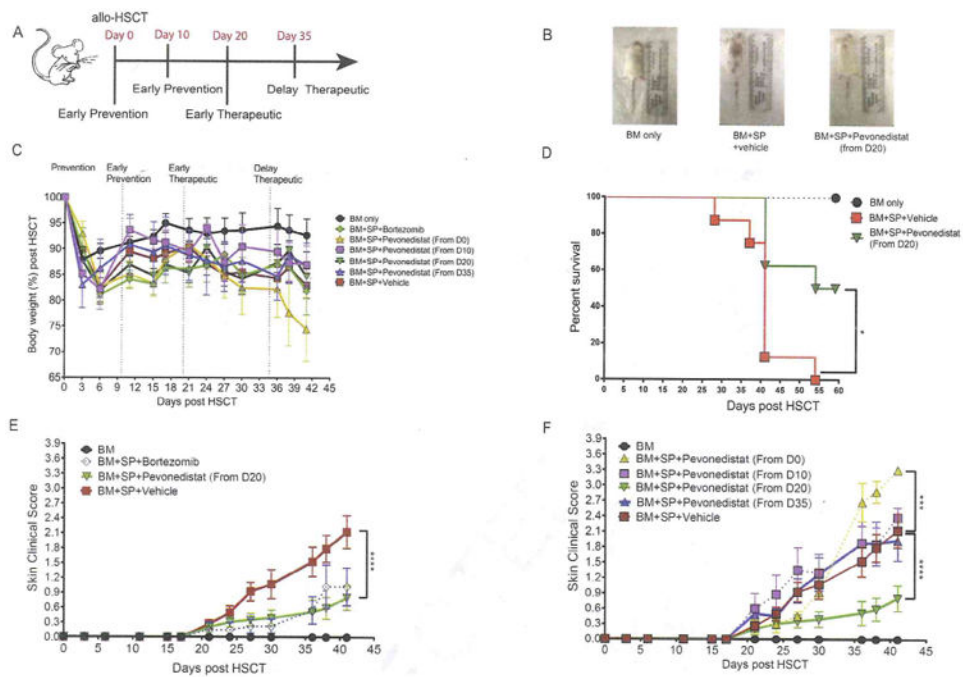


Figure 1. Time-dependent administration of pevonedistat produces differential scleroderma GVHD responses. Irradiated (8 Gy) BALB/c recipient mice underwent transplantation with BM cells with or without spleen cells (SP) from donor B10.D2 mice. Bortezomib was administered at day +20 and every 5 days thereafter, whereas pevonedistat was administered at the indicated times and every 5 days thereafter as well. (A) Scheme for pevonedistat or vehicle administration during cGVHD pathogenesis. (B) Representative pictures of mice that received BM cells only and BM cells and spleen cells with vehicle or pevonedistat from day 20. (C) Body weight changes among different regimen groups. (D) Survival rates in mice receiving BM only and BM cells and spleen cells with vehicle or pevonedistat from day +20. (E) Skin clinical score comparison among early therapy (from day +20) of bortezomib, pevonedistat, vehicle treatment, and BM-only groups. (F) Skin clinical score comparison among different pevonedistat administration times. Data, shown as mean \pm SEM, were analyzed by 2-way ANOVA among individual groups. Data are representative of 2 independent experiments with 4 to 8 mice per group. Significant P values: * P <.05; *** P <.001; **** P <.0001.

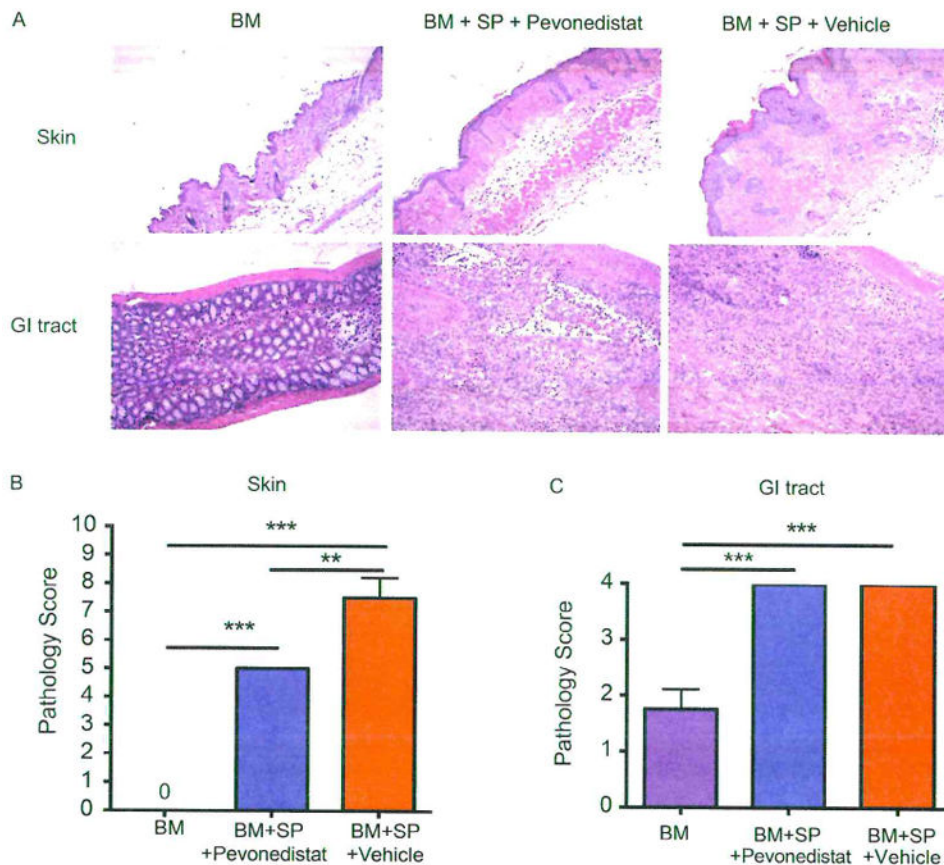


Figure 2. Histopathological analysis of mice that received pevonedistat treatment. Irradiated (8 Gy) BALB/c recipient mice underwent transplantation with BM cells with or without spleen cells (SP) from donor B10.D2 mice. Pevonedistat was administered i.p. at day +20 and every 5 days thereafter. Organs were harvested on day +59 after allo-HSCT. (A) Pathological examination of skin (upper) and GI tract (lower) by H & E stain. (B and C) Pathological scores for skin (on a scale of 0 to 10) and GI tract (on a scale of 0 to 4) were evaluated by pathologists in blinded fashion. Data, shown as mean±SEM, were analyzed by 1-way ANOVA with a Tukey post hoc test to compare individual groups. Data are representative of 2 independent experiments with 3 to 4 mice per group. Significant *P* values: ***P*<.01; ****P*<.001.

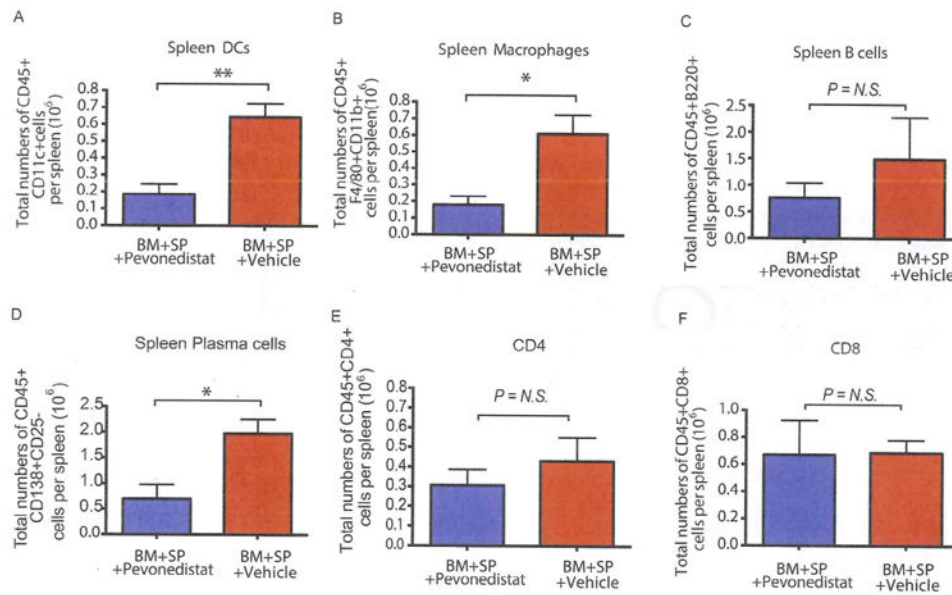


Figure 3.

Immune subsets after pevonedistat treatment. Irradiated BALB/c mice the underwent transplantation with BM and spleen cells (SP) were injected with either pevonedistat (20 mg/kg) or vehicle control starting at day +20. Spleen cells were collected at +day 59 after allo-HSCT. All cell subsets were gated as Ly9.1⁻ to distinguish donor-derived cells. (A) Total number of dendritic cells. (B) Total number of macrophages. (C) Total number of B cells. (D) Total number of plasma cells. (E) Total number of CD4 T cells. (F) Total number of CD8 T cells. The data, shown as mean \pm SEM, were analyzed with the Student *t* test to compare individual groups. Data are representative of 2 independent experiments with 4 to 8 mice per group. Significant *P* values: **P*<.05; ***P*<.01. N.S., non-significant.

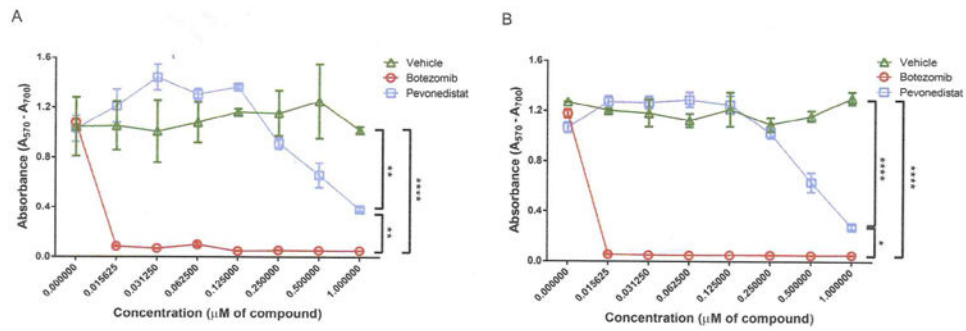


Figure 4.

Comparison of T cell inhibition by bortezomib and pevonedistat. Splenocytes from resting BALB/c mice were plated in 96-well plates and stimulated with concanavalin A (2 µg/mL) for 24 hours (A) or 48 hours (B) with vehicle (10% 2-hydroxy-propyl-beta cyclodextrin), the dosage range of bortezomib, or pevonedistat. Cell proliferation was determined with the MTT assay kit following the manufacturer's instructions. Cell proliferation was measured by the optical density at a wavelength of 570 nm. The reference wavelength was 700 nm. The data, shown as mean ± SEM, were analyzed by 2-way ANOVA to compare individual groups. Significant *P* values: **P*<.05; ***P*<.01; *****P*<.0001.

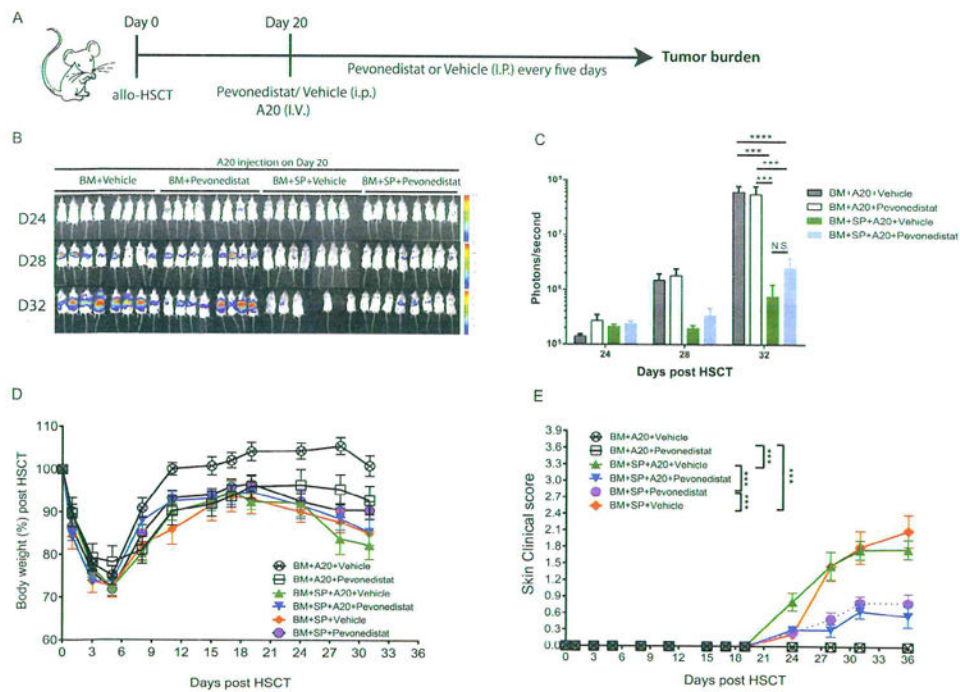


Figure 5. The impact of pevonedistat administration on cGVHD and GVT in the A20 tumor model. Irradiated BALB/c mice underwent transplantation with BM cells with or without spleen cells (SP) at day 0. A20 luciferase-transfected lymphoma cells (1×10^6) were injected through the tail vein into the indicated groups at day +20. Pevonedistat was also administered at day +20 and every 5 days thereafter. (A) Timeline schema for different conditions among groups. (B) Bioluminescence images acquired to monitor tumor burdens. (C) Quantification of tumor burden by bioluminescence signals. (D) Body weight changes after allo-HSCT. (E) Skin clinical scores were evaluated twice weekly. Data were collected from 1 experiment with 8 mice per group. The data, shown as mean \pm SEM, were analyzed by 2-way ANOVA for comparisons among individual groups. Significant P values: *** P < .001; **** P < .0001. N.S., nonsignificant.